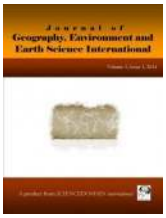

Journal of Geography, Environment and Earth Science International

12(4): 1-12, 2017; Article no.JGEESI.37283
ISSN: 2454-7352

Monitoring of Actual Evapotranspiration Using Remotely Sensed Data under Modern Irrigation Systems

M. A. El-Shirbeny[1*], A. M. Ali[1], E. S. Mohamed[1], K. Abutaleb[1,2] and S. M. Saleh[3]

[1]National Authority for Remote Sensing and Space Sciences (NARSS), Egypt.
[2]Institute for Soil, Climate and Water, ARC, Pretoria, South Africa.
[3]Central Laboratory for Agricultural Climate (CLAC), ARC, Egypt.

Authors' contributions

This work was carried out in collaboration between all authors. Authors MAES, AMA, ESM designed the study, collected the field data, analyzed the data and wrote the first draft of the manuscript. Authors KA and SMS managed the analyses of the study, managed the literature searches and revised and edited the first draft. All authors read and approved the final manuscript.

Article Information

DOI: 10.9734/JGEESI/2017/37283
Editor(s):
(1) Pere Serra Ruiz, Department of Geography, Universitat Autònoma de Barcelona, Spain.
Reviewers:
(1) Yong Chen, Texas A&M University, USA.
(2) Ružica Stričević, University of Belgrade, Serbia.
Complete Peer review History: http://www.sciencedomain.org/review-history/22007

Original Research Article

Received 9th October 2017
Accepted 14th November 2017
Published 21st November 2017

ABSTRACT

Agriculture monitoring and managements is a key factor in the food production and food security. Mainly, crop identification and area quantification are most important factors in yield estimation and predictions. In arid lands, water is a limiting factor for the agriculture expansion and development. Conventional methods for both crop discrimination and crop water requirements are very expensive and unbearable economically. Remote sensing has been employed several decades ago in the different agricultural activities. Crop discrimination, water requirements and even weed and pest control could be achieved via remote sensing and geographical information systems. This paper utilizes remote sensing data in combination with ground meteorological data to calculate the Actual Crop Evapotranspiration (ET_a) under modern irrigation systems conditions. Moreover, it also tries to discriminate between different crops and calculate area per crop type. Four Landsat8-OLI images were used to calculate the Land Surface Temperature (*LST)* during the different growth stages of

**Corresponding author: E-mail: mshirbeny@yahoo.com, m.elshirbeny@narss.sci.eg;*

the 2014 winter corps season. The dates of these satellite images were chosen to fall in the different growth stage of the crops in the study area. Ground meteorological data were used to estimate Reference Evapotranspiration (ET_o) using the FAO Penman-Monteith (*FPM*) equation. Land surface temperature and Air Temperature (T_{air}) were used to observe the water distribution conditions of the study area by the means of mapping the Water Deficit Index (*WDI*). The WDI and Potential Crop Evapotranspiration (ET_c) were used to calculate ET_a. The supervised maximum likelihood classification method was employed for crop mapping using spectral signatures collected from different ground training sites through different field visits during the growing stages of the growing season. The use of multi-temporal Normalized Difference Vegetation Index (NDVI) resulted in a classification accuracy of 93% with a kappa coefficient of 0.90. The crop water requirement was affected by the decreasing surface and air temperature. Crop type and different growth stages were detected through applying Multi-temporal images.

Keywords: Crop discrimination; Landsat8; potential-crop-evapotranspiration (ETc); reference-evapotranspiration (ETo); water-deficit-index (WDI).

1. INTRODUCTION

The advancements in satellite, airborne and ground based remote sensing, remotely sensed data are tremendously being used in agriculture. The use this data were evaluated in many agriculture activities. Many studies investigated the potentiality of remote sensing data in crop monitoring, yield prediction, weed control and pest management and crop water requirements [1-7]. [8] predicted soil water availability for irrigation water management by the use of remotely sensed data. Remote sensing estimation of Evapotranspiration (*ET*) can help detect, map and provide guidance for crop water requirements in irrigated lands [9]. It is also very beneficial in monitoring water stress in precision agriculture [10]. [11] developed the *Water Deficit Index (WDI)* that uses the remotely sensed *Land Surface Temperature (LST)*, T_{air} and vegetation index to estimate field relative water status. The *WDI* is a function of Actual Crop Evapotranspiration (ET_a) to Potential Crop Evapotranspiration (ET_c) ratio [12]. Yield water stress response depends on crop type and the phonological stage, soil, climatic conditions. The use of WDI in yield predictions or irrigation managements requires estimation of WDI for that particular crop under different soil, growth stage and climatic conditions [13]. Many satellite data were used to calculate *WDI* such as Landsat, Advanced Very High Resolution Radiometer (NOAA/AVHRR), and Moderate Resolution Imaging Spectroradiometer (*MODIS)*. [3] used *NOAA/AVHRR* to calculate *WDI* in the eastern part of Nile delta-Egypt. A *MODIS* index based on the spatial relationship between *LST* and Normalized Difference Vegetation Index (NDVI) was evaluated by [14] to estimate *WDI* in two sites with different climatic controls on ET_a in Andalusia-Spain. It is found that accounting for the spatial variation in T_{air} is one of the most critical factors to achieve accurate estimations of the Temperature–Vegetation Dryness Index (*TVDI*).

Several image classifiers are implementing in the different software packages such as the Maximum Likelihood, nearest neighbor, and minimum distance. These classifiers are used to group similar objects in thematic classified maps [15]. There are two types of these classifiers, supervised and unsupervised classifier. The unsupervised classifier do not require a prior knowledge about the study area while, the supervised one requires a prior knowledge of the concerned region. Prior knowledge about the study area could be via the selection of representatives training sites defined by the analyst having the knowledge about land cover and spectral characteristics of the region. These training sites would be used to train the classification algorithm. Different classifiers were compared to determine their performance under different situations and conditions. [15] compared the unsupervised ISODATA and the supervised Maximum likelihood to each other. He found that both of the two methods preforms well defining the spatial context. While, [16] reported the main disadvantage of Maximum likelihood is the prior knowledge of the distribution functions of the information classes, which is not possible to know the distribution functions.

Many authors confirmed the inaccuracies associated with crop discrimination depending on single date remotely sensed data. They also pointed out the use of multi-temporal remote sensing data corresponding to different growth stages was efficiently in crops identification and

discrimination [17-19]. Several researchers had discussed different methods to assess the accuracy of remotely sensed data [20]. However, the most widely used accuracy measures are derived from the confusion or the error matrix [21].

The main objectives of the current study are estimating the crop water status under pivot and drip irrigation using remotely sensed data as well as, crop discrimination using the multi-temporal Landsat8 images analysis.

2. MATERIALS AND METHODS

2.1 The Study Area

The study area is located in the eastern part from Nile Delta. It is called El-Salhia project as shown in Fig. 1. The irrigation systems exist in the project are mainly two systems, the central pivots and the drip irrigation system. It has about 100 pivot units. Each unit irrigates an area of about 63.6 *ha*. The common pivot length is about 450 m. Central pivots are particularly allocated for grain and cash crops such as vegetables, grain and silages while the drip irrigation system is mainly for trees.

2.2 Data Collection

Four Landsat 8 satellite images (path 176/row 039) were downloaded from the internet to cover the winter crops season. The acquisition dates of these images are 10 of Jan 2014, 11 Feb 2014, 15 Mar 2014 and 31 Mar 2014. These images were unzipped and stacked using image processing packages for further processing. Meteorological data were obtained from the closest available weather station in the study area. It includes air temperature, relative humidity, wind speed, and wind direction in the format of mean, minimum and maximum hourly readings. The hourly readings are averaged in daily mean for the corresponding satellite date.

2.3 Data Processing

2.3.1 *NDVI* and crop coefficient (*Kc*) estimation

Landsat8 bands 4 and 5 provide red (*R*) and near-infrared (*NIR*) measurements and therefore can be used to generate *NDVI* with the following formula:

NDVI = (Band 5 - Band 4) / (Band 5 + Band 4) (1)

The relation between *Kc* and *NDVI* represented by equation (2), which established by [22] and calibrated for wheat by [23].

$$Kc = \frac{1.2}{NDVI_{dv}}(NDVI - NDVI_{mv}) \quad (2)$$

Where 1.2 is the maximum Kc under Egyptian conditions, $NDVI_{dv}$ is the difference between the minimum and the maximum NDVI value for vegetation and $NDVI_{mv}$ is the minimum NDVI value for vegetation.

2.3.2 LST estimation

The recorded digital numbers of Band 10 was converted to radiance units (*Rad*) as follow:-

Rad = 0.0003342* *DN*+ 0.10000 (3)

Where DN is the pixel Digital Number

Land-Surface-Emissivity (*e*) was estimated according to the proportion of vegetation (*Pv*).

e = 0.004 *Pv* + 0.986 (4)

To apply this equation, the NDVI values for vegetation and soil are needed.

$$Pv = \left[\frac{NDVI - NDVIs}{NDVIv - NDVIs}\right]^2 \quad (5)$$

Where NDVI, $NDVI_S$ and $NDVI_V$ are the pixel, the minimum and the maximum NDVI values respectively.

The brightness temperature (*BT*) was calculated depending on band 10 radiance (*Rad10*) using calibration constants *K1*=774.89 and *K2*=1321.08.

BT = (*K2*/ Ln((*K1*/*Rad10*) +1)) -272.15 (6)

LST = BT/1+W*(BT/p)*Ln (e) (7)

Where BT is the at sensor temperature, W=Wavelength of emitted radiance (11.5µm), p = h*C/S ($1.438*10^{-2}$ mk), h = Planck's Constant ($6.626*10^{-34}$ JS), S = Boltzmann Constant ($1.38*10^{-23}$ J/K), C = Velocity of light ($2.998*10^{8}$ m/s), p = 14380.

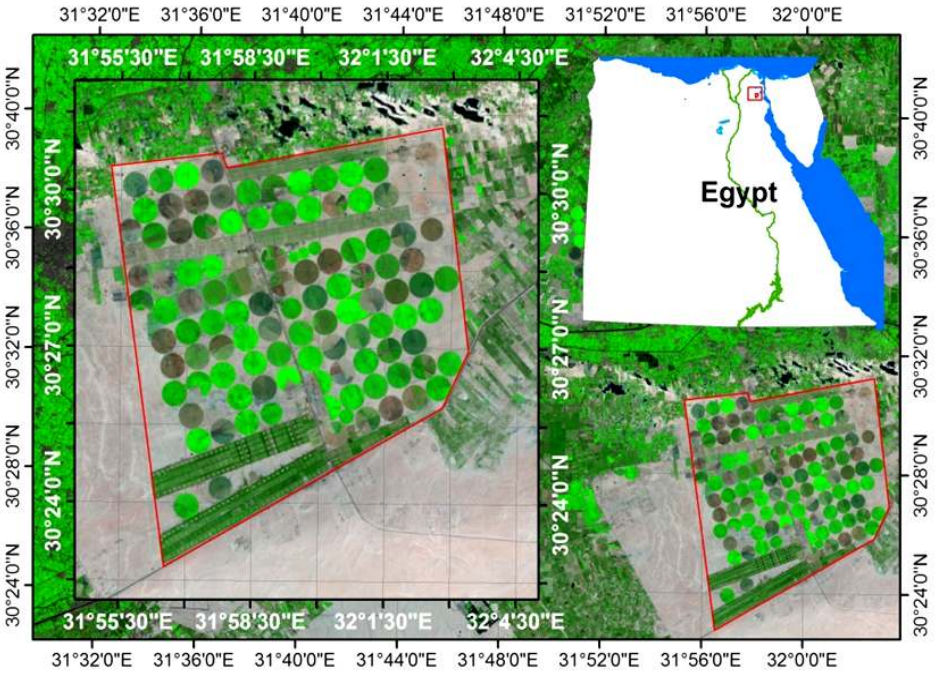

Fig. 1. Location map of the study area

2.3.3 ET_o and ET_c estimation

ETo was calculated from meteorological data using *FAO Penman equation (FPM)* method (equation 8) which prepared by [24].

$$ET_o = \frac{0.408\Delta(R_n - G) + \gamma\frac{900}{T+273}u_2(e_s - e_a)}{\Delta + \gamma(1 + 0.34u_2)} \quad (8)$$

Where R_n, net-radiation at the crop surface [*MJ m*$^{-2}$ *day* $^{-1}$], *G*, soil-heat-flux-density [*MJ m*$^{-2}$ *day* $^{-1}$], *T*, mean daily T_{air} at 2 *m* height [℃], u_2 ,wind speed at 2 *m* height [*m s*$^{-1}$], e_s, saturation-vapor-pressure [*kPa*], e_a, actual-vapor-pressure [*kPa*], *es - ea*, saturation-vapor-pressure deficit [*kPa*], Δ, slope-vapor-pressure curve [*kPa* ℃ $^{-1}$], γ, psychrometric constant [*kPa* ℃ $^{-1}$].

Equations (2) and (8) were used to estimate (*ETc*) as shown in equation (9).

$$ET_c = ET_o * Kc \quad (9)$$

2.3.4 *WDI* and ET_a estimation

The *WDI* was developed by [11]. It depends on *LST*, T_{air} and vegetation-index. It could be calculated as illustrated by equation (10). It gives an estimate of the relative-water-status for the study area.

$$WDI = \frac{\Delta T - \Delta Tm}{\Delta Tx - \Delta Tm} \quad (10)$$

Where ΔT is the difference between *LST* and T_{air}, ΔTm is the difference between LST_{min} and T_{air}, ΔTx is the difference between LST_{max} and T_{air}.

The *WDI* considers evaporation from the soil surface as well as the crop. It can be interpreted as a measure of the amount of *ET* actually occurring relative to the ET_c (equation 11).

$$WDI = 1 - ET_a/ET_c \quad (11)$$

2.4 Crop Discrimination and Accuracy Assessment

Maximum likelihood supervised classification technique was used to perform multi-temporal crop area identification using the *NDVI* signature extracted from a combinations of the four different Landsat8 images and four Landsat 7 images. It was very useful to get a full NDVI spectrum during the growing season and give insights to select the probable dates for crop discrimination based on the NDVI. Dates were selected to represent the agricultural activity period for the selected study area. Training sites with known crops were used to extract pure signatures. Four *NDVI* composites were used for the season of 2014 winter crops to determine the crop cycle for these crops,

discriminate different crops and calculate the area.

Accuracy assessment was carried out by the mean of confusion matrix and kappa coefficient. The confusion matrix is a simple cross-tabulation of the mapped class label against that observed in the ground or reference data for a sample of cases at specified locations [21].

A number of 100 random points were selected to generate accuracy assessment report of classification. These points were representative of each different class and the number of points was selected considering the size of the study area and available ground truth data.

3. RESULTS AND DISCUSSION

3.1 Potential Crop Evapotranspiration (ET_c)

Many researchers used *FPM* method to estimate ET_o from the ground meteorological data to evaluate or to couple it with remotely sensed data. In the current study, ET_o values varied from 1.5 *mm/day* to 3.3 *mm/day* during study season. ET_o values were 1.5, 2.3, 2.8 and 3.3 *mm/day* on Jan. 10th, 2014, Feb. 11th, 2014, Mar. 15th, 2014 and Mar. 31st, 2014 respectively.

Kc was first fully implemented by relating *ET* for a given crop over a specific period, which called ET_c as the rate of *ET* from a non-water-stressed crop having an aerodynamically rough surface like grass or alfalfa with 0.3-0.5 *m* [25].

The *Kc* was stated to represent the combined effects of resistance to water movement from the soil to the evaporating surfaces, resistance to diffusion of water vapor from the evaporating surfaces through the laminar boundary layer, resistance to turbulent transfer to the free atmosphere, and relative amount of radiant energy available as compared to the reference crop [26, 27].

Kc value depends on the stage of canopy height, crop growth, architecture, and cover [24, 28]. The *Kc-NDVI* relationship is highly correlated. Many parameters are affecting on *NDVI* values such as; planting density, crop age, and chlorophyll activity. The results of *Kc* values varied in study area according to Landsat8 data from 0 to 1.2, while the ET_c values varied from 0 to 3.7 *mm/day* according to land cover type, crop stage and weather conditions as shown in Fig. 3.

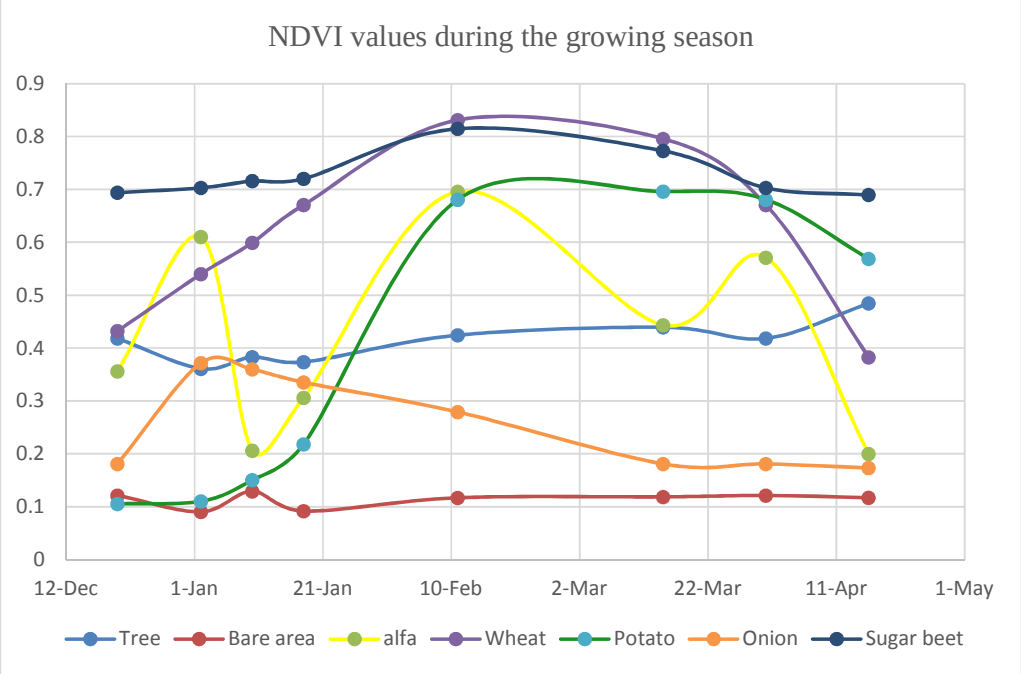

Fig. 2. NDVI for the existing crops during the winter seasons

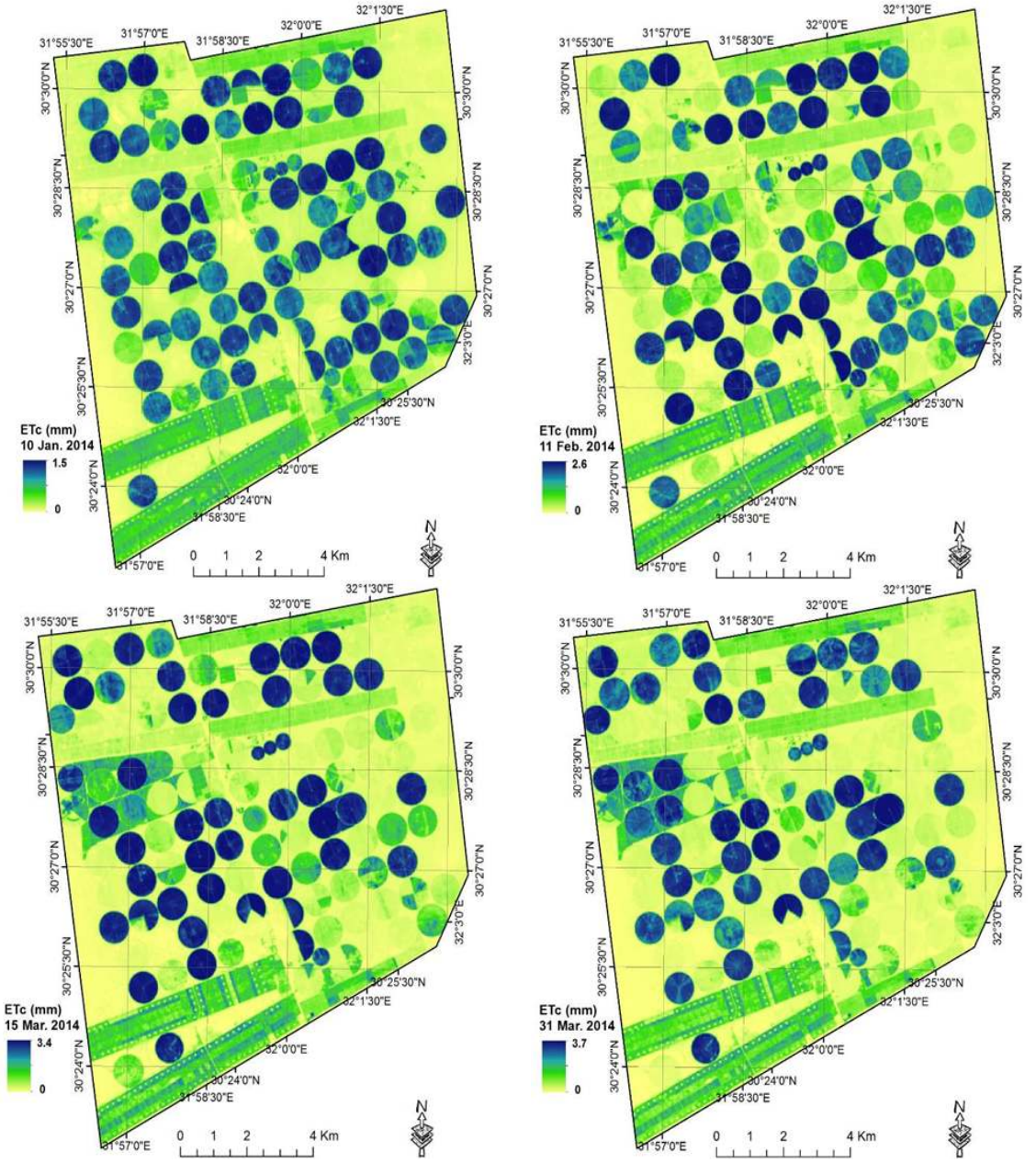

Fig. 3. ET_c distribution in study area

3.2 Water Deficit Index (*WDI*)

The canopy temperature is an indicator of vegetation water stress. When plants suffer from water shortages accordingly, stomata close to reduce or even stop transpiration as an adaptation step, which will increase the leaf temperature [29]. [11] developed the WDI to count for the soil background which is sometimes mislead to vegetation water stress in the early growing stages due to the partial plants cover. The *WDI* depends mainly on LST and T_{air}. It has minimum value of zero of the indicating no water stress, and a maximum value of one represents maximum water stress.

Fig. 4 represents the spatial distribution for the *WDI* over the study area. It is clear that the bare soil has a very high *WDI* since it is almost dry while the central pivots have low values of *WDI*. The values of the cultivated areas ranged between 0 and 0.5 according to the growth

stage, water shortage and crop cover percentage. Hence, at the early growth stage, the crop cover is partially and soil contributes more to the net *WDI* values so it appears by the yellow color. In fact *WDI* can tell many useful information not only the water status of the crop but also it can tell the current development stage of the growing crop via multi-temporal satellite based *WDI* over the entire season. In the current study, one can find some pivots at January with

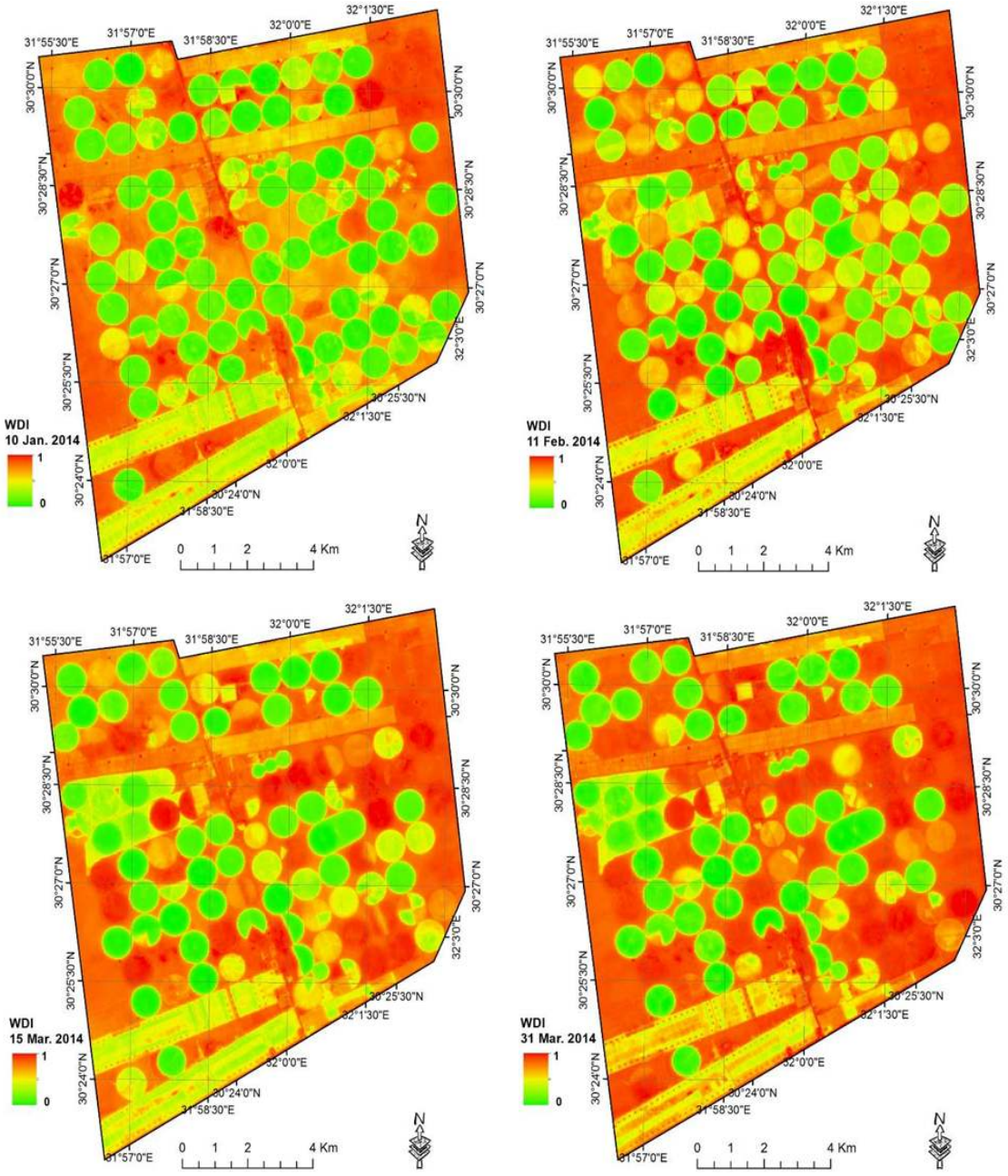

Fig. 4. *WDI* distribution in the study area

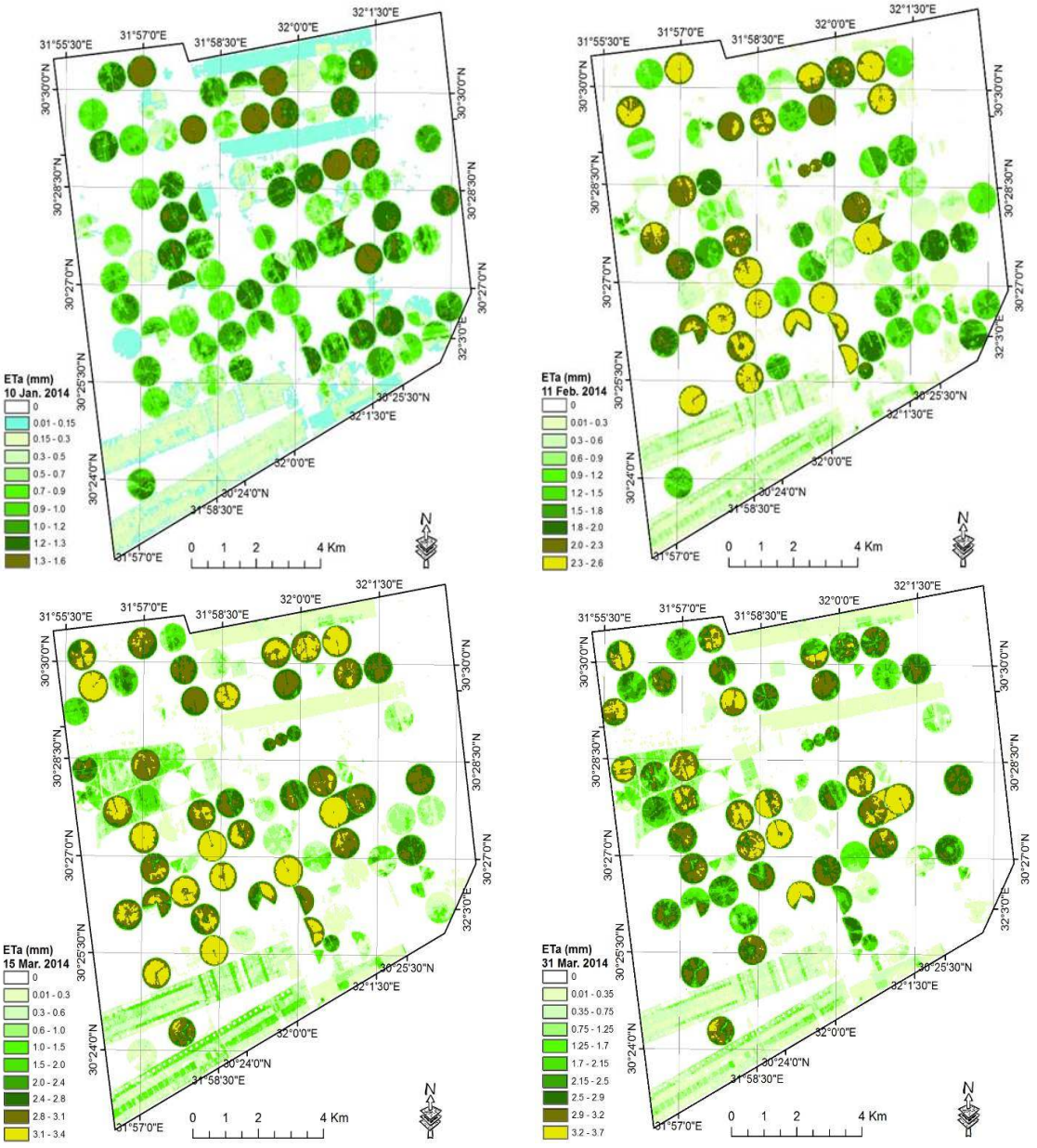

Fig. 5. *ETa* distribution in study area

low values of WDI while these values start to increase consequently in following months. The wise interpretation of these results must lead to the fact that these pivots tends to the harvesting stage. On the other hand, if the pivot starts with high values of *WDI* and tends to decrease consequently it indicates the start of growing a new crop. Other useful information could be extracted from the multi-temporal *WDI* investigation is the crop type i.e. biannual, annual or a dominant crop such as tress.

3.3 Actual Evapotranspiration (ET_a)

ET_a can be estimated by many models which vary in complexity but the accuracy of ET_a estimation is proportional to the degree of calibration and validation of the used model or sub-models. [30] categorized the ET_a estimation into three groups of methods: 1. Methods based on analytical modeling of *ET*; 2. Methods use the deduction from the *ET* of a reference surface; 3. Methods based on a soil water balance modeling.

In arid and semi-arid climates, *ET* ranges over a large interval depending on water regimes. Moreover, the variation in one weather parameter immediately influences all the other variables that are mutually related. This fact makes difficult to correctly evaluate the ET_a [30].

Er-Raki [31] have analyzed the efficiency of three methods based on the FAO-56 *Kc* approach to estimate ET_a for winter wheat under different irrigation treatments in the semi-arid conditions of Morocco.

ET_a (*mm/day*) is the product of an uptake coefficient (α, *mm/day*) and available water ($\theta - \theta WP$) when ET_a is less than ET_c (*mm/day*): If $ET_a < ET_c$, $ET_a = \alpha\ (\theta - \theta WP)$ and If $ET_a \geq ET_c$, $ET_a = ET_c$. ET_c occurs when the availability of soil water does not limit transpiration [32] and it could be estimated using the *FPM* model [24].

In the current study the values of ET_a varied from 0 to 3.7 *mm/day*. ET_a was affected by the changing in *WDI* and ET_c according to Equation (11). As shown in Fig. 5, the variation of ET_a was observed according to land cover type, crop stage, weather conditions and water stress conditions.

3.4 Crop Discrimination and Accuracy Assessment

The classification of multi-temporal images gives valuable information on agricultural activities in terms of crop type identification and crop area identification. The multi-temporal variability of profiles was assessed by analyzing the multi-temporal *NDVI* differences among season. This approach has been used in many studies using *NDVI* from *NOAA/AVHRR* and *MODIS* images [33,34]. Classification procedure runs with the use of homogenously distributed signatures that are associated with training sites and the result is the determination of information classes [35].

This classification approach was evaluated with accuracy assessment procedure and visual interpretation of the result images based on ground truth information. According to the accuracy assessment results, the supervised classification of four multi *NDVI* image overall classifications accuracy was 93% and kappa value was 0.90. Classification results are shown in Fig. 6 and the area of the different classes are shown in Table 1.

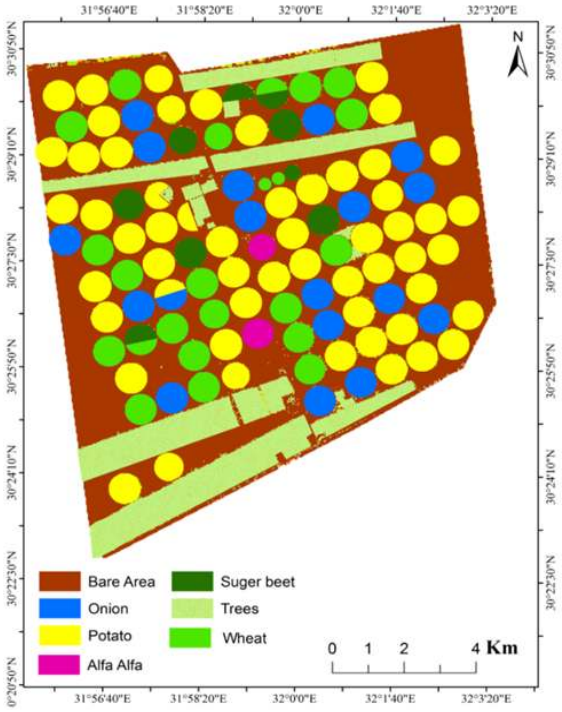

Fig. 6. Supervised classifications using multi-temporal *NDVI*

Table 1. Total area (Feddans) of the different winter crops in study area (season 2014)

Wheat	Potato	Onion	Alfa	Sugar beet	Bare area	Trees
2825.871	7951.551	2549.408	111.8614	807.1021	10742.43	5347.107

As shown, the classification results of El-salhia site that almost 35.4% of the total area was temporary non-vegetated areas during the winter season. Largest vegetated area (almost 25% of the total area) was cultivated by potato followed by trees that occupy 17.62% of the total area. On the other hand wheat and sugar beets represented by 9.3 % and 2.66 % respectively.

4. CONCLUSIONS

The study was carried out in El-Salhia project which located in eastern part of Nile delta, Egypt. The extensive use of modeling techniques in water resources management increases the demands of more spatial and temporal data for modeling accuracy and validity improvements. Four Landsat8 scenes were acquired on Jan. 10th, 2014, Feb. 11th, 2014, Mar. 15th, 2014 and Mar. 31st, 2014. *NDVI* and *LST* were extracted from Landsat8 satellite data and used with T_{air} to estimate *WDI*. The *Kc* was derived from remotely sensed data depending on *NDVI.* The integration of *FPM* model with remotely sensed data was able to detect ET_c. The results showed that the ET_o varied from 1.5 to 3.3 *mm/day* where ET_c and ET_a varied between 0 and 3.7 *mm/day* during the study period. As a result, the planning for irrigation strategies will be easier with approaches which use remotely sensed derived parameters. It could be a useful and low-cost method for estimating crop water requirements and enhancing water resources management, especially in arid and semi-arid regions.

COMPETING INTERESTS

Authors have declared that no competing interests exist.

REFERENCES

1. Rwasoka DT, Gumindoga W, Gwenzi J. Estimation of actual evapotranspiration using the Surface Energy Balance System (SEBS) algorithm in the Upper Manyame catchment in Zimbabwe. Physics and Chemistry of the Earth. 2011;36:736–746. Available:https://doi.org/10.1016/j.pce.2011.07.035
2. Merlin O, Chirouze J, Olioso A, Jarlan L, Chehbouni G, Boulet G. An image-based four-source surface energy balance model to estimate crop evapotranspiration from solar reflectance/thermal emission data (SEB-4S). Agricultural and Forest Meteorology. 2014;184:188–203. Available:https://doi.org/10.1016/j.agrformet.2013.10.002
3. El-Shirbeny MA, Aboelghar MA, Arafat SM, El-Gindy AGM. Assessment of the mutual impact between climate and vegetation cover using NOAA-AVHRR and Landsat data in Egypt, Arabian Journal of Geosciences, 2014a;7(4):1287-1296. Available:https://doi.org/10.1007/s12517-012-0791-3
4. El-Shirbeny MA, Saleh NH, Ali AM. Estimation of potential crop evapotranspiration using remote sensing techniques. Proceedings of the 10th International Conference of AARSE. 2014b;460–468.
5. Hu G, Jia L, Menenti M. Comparison of MOD16 and LSA-SAF MSG evapotranspiration products over Europe for 2011. Remote Sensing of Environment. 2015;156:510–526. Available:http://dx.doi.org/10.1016/j.rse.2014.10.017
6. Tadesse T, Senay GB, Berhan G, Regassa T, Beyen S. Evaluating a satellite-based seasonal evapotranspiration product and identifying its relationship with other satellite-derived products and crop yield: A case study for Ethiopia. International Journal of Applied Earth Observation and Geoinformation. 2015;40:39–54. Available:http://dx.doi.org/10.1016/j.jag.2015.03.006
7. Wojtowicz M, Wojtowicz A, Piekarczyk J. Application of remote sensing methods in agriculture. Communications in Biometry and Crop Science. 2016;11:31–50.
8. Oki T, Kanae S. Global hydrological cycles and world water resources. Science. 2006;313:1068-1072.
9. French AN, Hunsaker DJ, Thorp KR. Remote sensing of evapotranspiration over cotton using the TSEB and METRIC energy balance models. Remote Sensing

of Environment. 2015;158(2015):281–294. Available:http://dx.doi.org/10.1016/j.rse.2014.11.003

10. Ghulam A, Li Z, Qin Q, Yimit h, Wang J. Estimating crop water stress with ETM+ NIR and SWIR data. Agricultural and Forest Meteorology. 2008;148:1679–1695. DOI: 10.1016/j.agrformet.2008.05.020
11. Moran MS, Clarke TR, Inoue Y, Vidal A. Estimating crop water deficit using the relation between surface air temperature and spectral vegetation index, Remote Sens. Env. 1994;49:246-263. Available:https://doi.org/10.1016/0034-4257(94)90020-5
12. Hiler EA, Clark RN. Stress day index to characterize effects of water stress on crop yields, Transactions of Hydrology (210-VI-NEH); 1971.
13. Erdem Y, Sehirali S, Erdem T, Kenar D. Determination of crop water stress index for irrigation scheduling of bean (*Phaseolus vulgaris L*.). Turkish Journal of Agriculture and Forestry. 2006;30:195-202.
14. Garcia M, Fernández N, Villagarcía L, Domingo F, Puigdefábregas J, Sandholt I. Accuracy of the temperature–vegetation dryness index using MODIS under water-limited vs. energy-limited evapotranspiration conditions, Remote Sensing of Environment. 2014;149:100–117. Available:http://dx.doi.org/10.1016/j.rse.2014.04.002
15. Harris R. Remote sensing of agriculture change in Oman. International Journal of Remote Sensing. 2003;24(23):4835–4852. Available:http://dx.doi.org/10.1080/0143116031000068178
16. Omkar SN, Senthilnath J, Mudigere D, Kumar MM. Crop classification using biologically-inspired techniques with high resolution satellite image. Journal of Indian Society of Remote Sensing, 2008;36:175-182. Available:https://doi.org/10.1007/s12524-008-0018-y
17. Murthy CS, Raju PV, Badrinath KVS. Classification of wheat crop with multi-temporal images: performance of maximum likelihood and artificial neural networks, International Journal of Remote Sensing, 2003;24(23):4871–4890. Available:http://dx.doi.org/10.1080/0143116031000070490
18. Karjalainen M, Kaartinen H, Hyyppä J. Agricultural monitoring using ENVISAT alternating polarization SAR images. Photogrammetric Engineering & Remote Sensing. 2008;74(1):117-126. Available:https://doi.org/10.14358/PERS.74.1.117
19. Tavakkoli Sabour SM, Lohmann P, Soergel U. Monitoring agricultural activities using multi-temporal ASAR ENVISAT Data: IntArchPhRS. Band XXXVII, Teil B7-2. Peking, S. 2008;735-742.
20. Congalton RG, Green K. Assessing the accuracy of remotely sensed data: principles and practices. Boca Raton, Lewis Publishers; 1999.
21. Foody GM. Status of land cover classification accuracy assessment. Remote Sensing of Environment. 2002; 80:185-201. Available:https://doi.org/10.1016/S0034-4257(01) 00295-4
22. El-Shirbeny MA, Ali A, Saleh N. Crop water requirements in egypt using remote sensing techniques. Journal of Agricultural Chemistry and Environment. 2014c;3:57-65. DOI: 10.4236/jacen.2014.32B010.
23. El-Shirbeny MA, Ali AM, Badr MA, Bauomy EM. Assessment of wheat crop coefficient using remote sensing techniques. World Research Journal of Agricultural Sciences. 2014d;1(2):12-17.
24. Allen RG, Perrier LS, Raes D, Smith M. Crop evapotranspiration: guidelines for computing crop requirements. FAO Irrigation and drainage, paper No. 56, Rome, Italy; 1998. Available:http://www.fao.org/docrep/X0490E/X0490E00.htm
25. Jensen ME. Water consumption by agricultural plants, In: Kozlowski, T.T. (Ed.), Water Deficits and Plant Growth, Vol. II. Academic Press, Inc., New York, NY. 1968;1–22.
26. Jensen CR, Battilani A, Plauborg F, Psarras G, Chartzoulakis K, Janowiak F, Stikic R, Jovanovic Z, Li G, Qi X, Liu F, Jacobsen S, Andersen MN. Deficit irrigation based on drought tolerance and root signalling in potatoes and tomatoes. Agricultural Water Management. 2010;98: 403-413. Available:https://doi.org/10.1016/j.agwat.2010.10.018
27. Pereira LS, Allen RG, Smith M, Raes D. Crop evapotranspiration estimation with

FAO56: Past and future. Agricultural Water Management. 2015;147:4–20.
Available:https://doi.org/10.1016/j.agwat.2014.07.031

28. Doorenbos J, Pruitt WO. Guidelines for predicting crop-water requirements, FAO Irrigation and Drainage, Paper No. 24, FAO, Rome, Italy; 1997.
Available:http://trove.nla.gov.au/version/13022899
29. Jackson RD, Idso SB, Reginato RJ, Pinter Jr. Canopy temperature as a crop water stress indicator. Water Res. 1981;17: 1133-1138.
DOI: 10.1029/WR017i004p01133
30. Rana G, Katerji N. Measurement and estimation of actual evapotranspiration in the field under Mediterranean climate: A review. European Journal of Agronomy. 2000;13:125–153.
Available:https://doi.org/10.1016/S1161-0301(00)00070-8
31. Er-Raki S, Chehbouni A, Guemouria N, Duchemin B, Ezzahar J, Hadria R. Combining FAO-56 model and ground based remote sensing to estimate water consumption of wheat crops in semi-arid regions. Agric. Water Manag. 2007;87:41–54.
32. Dardanelli JL, Ritchie JT, Calmon M, Andrianiand JM, Collino DJ. An empirical model for root water uptake. Field Crops Research. 2004;87:59-71.
Available:https://doi.org/10.1016/j.fcr.2003.09.008
33. Justice CO, Townshend JRG, Kalb VL. Representation of vegetation by continental datasets derived from NOAA-AVHRR data. International Journal of Remote Sensing, Basing Stoke. 1991;12: 999-1021.
Available:http://dx.doi.org/10.1080/01431169108929707
34. Zhang X, Friedl MA, Shaaf CB, Strahler AH, Hodges JCF, Gao F, Reed BC, Huete A. Monitoring vegetation phenology using MODIS. Remote Sensing of Environment, 2003;84:471-475.
Available:https://doi.org/10.1016/S0034-4257(02)00135-9
35. Kucukmehmetoglu M, Geymen A. Measuring the spatial impacts of urbanization on the surface water resource basins in Istanbul via remote sensing. Environmental Monitoring and Assessment. 2008;142:153–169.
DOI: 10.1007/s10661-007-9917-6

Peer-review history:
The peer review history for this paper can be accessed here:
http://sciencedomain.org/review-history/22007